Probing the Impact of Scale on Data-Efficient, Generalist Transformer World Models for Atari

Anonymous authors
Paper under double-blind review

Abstract

Developing generalist systems that retain human-like data efficiency is a central challenge. While world models (WMs) offer a promising path, existing research often conflates architectural mechanisms with the independent impact of model *scale*. In this work, we use a minimalist transformer world model to analyze scaling behaviors on the Atari 100k benchmark, using fixed offline datasets derived from a presupposed expert policy. Our results reveal that the scaling strategy is governed by the latent intrinsic dimensionality of the environment. For individual tasks, we identify distinct regimes: while low-complexity environments pass the interpolation threshold, yielding monotonic improvements, high-complexity dynamics remain in the classical regime, where larger models degrade performance. Conversely, in the unified setting, i.e., a single transformer trained on a suite of 26 Atari environments, we uncover a phenomenon of *positive regularization*: joint training stabilizes scaling dynamics, ensuring monotonic gains across all environments regardless of their intrinsic dimensionality. Finally, we demonstrate that improved fidelity translates directly to downstream control, with policies learned entirely within the simulated dynamics achieving a median expert-random-normalized score of 0.770. Our findings suggest that future progress lies as much in precise scaling strategies as in architectural innovation.

1 Introduction

The development of generalist artificial intelligence (AI)—a single system capable of mastering a diverse suite of tasks with a *unified* set of parameters—remains a central goal of AI research (Reed et al., 2022). While the emergence of foundation models has validated the potential of unified architectures to absorb behaviors across disparate modalities (Bommasani et al., 2021), these systems typically rely on experience accumulation that vastly exceeds biological learning timescales. This stands in stark contrast to human intelligence, which is characterized by the ability to grasp complex dynamics from limited interactions (Lake et al., 2015). Consequently, a critical challenge lies in bridging this gap: deriving architectures that possess the breadth of a generalist while retaining the strict data efficiency characteristic of human learning.

The Atari 100k benchmark serves as a critical testbed for this pursuit. Constrained to a total budget of 400k environmental frames, corresponding to 100k agent interactions with a frame skip of 4, the benchmark limits experience to roughly two hours of human gameplay, thereby qualifying as a strictly data-efficient setting. Furthermore, the benchmark offers a suite of distinctive dynamical systems across 26 games, demanding a diverse array of capabilities: from reaction speed in Asterix and motor precision in Freeway, to path-planning and spatial awareness in MsPacman, risk assessment in Seaquest, delayed gratification in Pong, and meta-learning mechanics without explicit instruction in Frostbite.

World models (WMs) (Ha & Schmidhuber, 2018a;b) offer a promising path toward such data-efficient, generalist AI. By learning a generative model of the environment, WMs enable planning within virtual rollouts, analogous to human imagination (Hamrick, 2019). This paradigm shifts the burden of sample complexity; environmental interaction is devoted solely to forming the model, while the extensive trial-and-error process of policy learning occurs entirely within the learned dynamics, incurring no real-world cost.

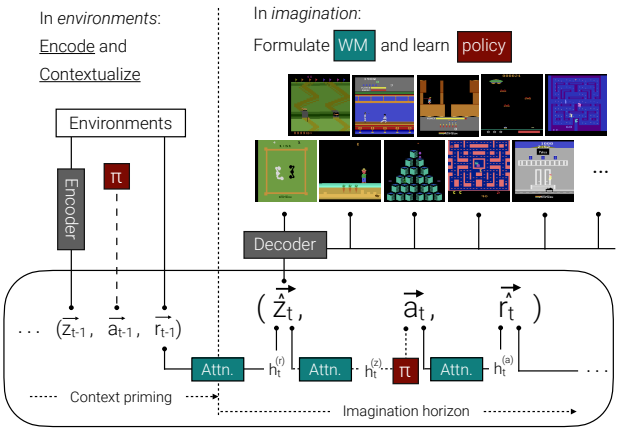

Figure 1: **Overview of the minimalistic world model. (Left)** We collect sequences of triplets (latent embeddings $\vec{z}_{t-1}$, actions $\vec{a}_{t-1}$, rewards $\vec{r}_{t-1}$) to construct a fixed offline dataset. No policy learning occurs during this interaction phase. **(Right)** Unrolling the imagination. Using the offline data as context, the model autoregressively generates future tokens $\hat{\vec{z}}_t$ and $\hat{\vec{r}}_t$, and the policy is learned inside the imagined, virtual rollouts to sample the action $\vec{a}_t$.

Consequently, a substantial body of work has proposed achieving data-efficient or generalist agents using WMs in the Atari domain. Aside from recent probabilistic approaches (Alonso et al., 2024), the dominant backbone for these systems remains the transformer (Vaswani et al., 2017). Methods such as the transformer world model (TWM) (Robine et al., 2023), IRIS (Micheli et al., 2023), and STORM (Zhang et al., 2023) have demonstrated remarkable data efficiency, while Multi-Game Decision Transformers (Lee et al., 2022) have explored generalist capabilities across large suites of gaming dynamics.

Despite this progress, the current landscape lacks a rigorous analysis of *scale*. Existing literature prioritizes novel architectural mechanisms and structural priors, yet their implementations, e.g., model depth, width, and context length, vary drastically (Refer to Appendix F for our summary). This conflation of methodological innovation with arbitrary scaling choices obscures the precise drivers of empirical improvements. Consequently, it remains unclear whether the performance saturation observed in complex environments stems from inherent architectural deficiencies or simply from operating within sub-optimal scaling regimes.

In this work, we adopt a minimalist approach to devise a transformer world model using standard, off-the-shelf components (section 3), allowing us to conduct a controlled analysis on the impact of scale for both individual (environment-wise) and unified world models (all 26 environments). Our primary findings are:

- In subsection 4.1, we establish a rigorous upper bound for performance by constructing a fixed offline dataset for each gaming environment using a presupposed expert policy. This allows us to evaluate the fidelity of the world model, which is formulated from the offline dataset, by measuring the precise degree to which a policy trained entirely within the learned dynamics recovers the presupposed expert capabilities.
- In subsection 4.2, we demonstrate that optimal scaling for individual world models is strictly governed by the intrinsic dimensionality of the specific environment. Even within a fixed offline data budget, environments exhibit distinct scaling behaviors; those with lower intrinsic dimensionality allow models to pass the interpolation threshold, resulting in monotonic performance improvements, while others remain trapped in a classical parameterization regime, i.e., *bigger models hurt*.
- In subsection 4.3, we examine the unified world model trained on all 26 games. We uncover a distinctive and unexpected form of *positive regularization*. In direct contrast to diverging scaling patterns observed in individual models, the unified training stabilizes the overall scaling behavior, ensuring that increasing model capacity, after surpassing the interpolation threshold, yields monotonic improvements across all individual tasks regardless of their intrinsic dimensionality, i.e., *bigger models never hurt*.
- In subsection 4.4, we demonstrate that the improved fidelity achieved solely through proper scaling—isolated from modeling idiosyncrasies—translates directly to effective downstream policy learning. We show that policies learned entirely inside our minimalist, properly scaled world models achieve mean and median normalized scores of 0.7490 and 0.770 relative to the expert upper bound and random lower bound with the exact same model configurations and environmental steps as the presupposed expert policy.

Overall, we highlight the critical role of scale in generative world models for achieving data-efficient generalist AI, suggesting that future progress may depend as much on scaling strategies as on architectural innovations.

2 Related work

World models (Ha & Schmidhuber, 2018a;b) learn to simulate environmental dynamics, enabling agents to plan actions based on synthesized future trajectories rather than through environmental interactions. Crucially, this paradigm extends to training agents entirely within the imagined Markov decision process (MDP) instantiated by itself—a process often referred to as learning in imagination (Hamrick, 2019).

To improve the training outcomes using the imagination MDPs, we need a stable world model that accurately mimics the real environment and generalizes well to yet unexplored parts of the world. The Dreamer models and their variants (Hafner et al., 2019; 2021; Ma et al., 2024; Hafner et al., 2025a) build on recurrent state-space models (RSSMs) to form world models and operate on continuous (DreamerV1) or discrete (DreamerV2, DreamerV3) latent representations. Notably, DreamerV3 uses fixed hyperparameter settings for different Atari games and other domains, but uses separate models (model parameters) and policy learning algorithms for different environments. Łukasz Kaiser et al. (2020) propose SimPLe that uses long short-term memory (LSTM) (Hochreiter & Schmidhuber, 1997) to model sequences of discrete latent representations.

Aside from the above models, Chen et al. (2022) propose transformers (Vaswani et al., 2017) as world model backbones. Micheli et al. (2023), Robine et al. (2023), Micheli et al. (2024), and Zhang et al. (2024b) propose transformer-based world models that outperform other model-based and model-free approaches on Atari 100k (Łukasz Kaiser et al., 2020) without lookahead search. Burchi & Timofte (2025) further advance this with TWISTER, incorporating contrastive predictive coding to enhance long-horizon consistency in transformer world models. Similarly, Agarwal et al. (2024) propose a transformer-based world model with discrete input tokens using a vector-quantized VAE (Van Den Oord et al., 2017) and use the decoder to retrieve inputs for the learning algorithm. A primary benefit of employing discrete embeddings via VQ-VAE, as seen in Micheli et al. (2023) and Agarwal et al. (2024), is the effective capture of visual details by distributing information over multiple tokens. Furthermore, discrete tokenization fits seamlessly into standard NLP transformers, mirroring the inherent discreteness of human language. The downside is slow inference in the world model, as generating multiple tokens per image results in an increased number of function evaluations (NFE). Alternatively, Hafner et al. (2021; 2025a); Robine et al. (2023); Zhang et al. (2024b) build upon the categorical encoder-decoder, which enhances generalization capability through latent sparsity (Hafner et al., 2021). When applied to transformer world models, it allows for assigning a single token per image observation (Zhang et al., 2024b), thereby reducing inference cost. Refer to Appendix B.1 for an extensive discussion on preserving the visual details in different world model architectures.

Departing from discrete tokenization, Hafner et al. (2025b) introduce DreamerV4, which utilizes a block-causal transformer operating on a grid of continuous latents. To overcome the inference bottleneck of autoregressive generation, they propose a diffusion-based objective termed shortcut forcing, a variant of the diffusion forcing (Chen et al., 2024), which enables the model to predict future states with flexible step sizes. This approach reconciles the trade-off between spatial fidelity and computational efficiency, allowing for real-time imagination of high-dimensional dynamics without the cost of sequential token prediction.

Lee et al. (2022) proposes the multi-game decision transformer that trains a single agent capable of solving multiple Atari games. They split a single image observation into patches and use uniform quantization for image tokenization. Contrary to our work, it requires hundreds of millions of data points or relies on human guidance to train a generalist agent. Nauman et al. (2024) demonstrate that increasing model capacity, combined with categorical value distributions and regularization, enables efficient multi-task learning on Atari. Similarly, Schwarzer et al. (2023) show that in the model-free setting (BBF), scaling the network depth and width is a primary driver of data efficiency, outperforming complex algorithmic modifications. Cheng et al. (2025) also highlight the importance of scale in the offline setting, proposing JOWA to jointly optimize world and action models for improved performance. Deng et al. (2023) adopt S4 models (Gu et al., 2022) that excels in modeling long-term dependencies and fast inference. Zhang et al. (2024a), Ding et al. (2024) and Alonso et al. (2024) concurrently propose diffusion (Ho et al., 2020)-based world models, which excel in capturing visual details at the cost of lacking the capability to model long-term dependencies.

In contrast to prior works that rely on novel inductive biases to enhance fidelity, we adopt a strictly minimalist design philosophy. We purposefully employ standard, off-the-shelf components to isolate the effects of model scale necessitated by diverse Atari gaming environments. This work thus serves as a validation of model scale rather than architectural idiosyncrasies in the regime of data-efficient generalist world models.

3 Method

We consider a multi-environment Markov decision process (MEMDP) (Raskin & Sankur, 2014), which generalizes a partially observable Markov decision process (POMDP) (Kaelbling et al., 1998; Sutton & Barto, 1998) to a setting with distinct underlying dynamics. Formally, an MEMDP is defined as a tuple $\langle \mathbb{S}, \mathbb{A}, \mathbb{O}, \{T_k\}_{k=1}^{K}, R, Z, \gamma \rangle$. Here, $\mathbb{S}$ denotes a set of states, $\mathbb{A}$ is a set of discrete actions, and $\mathbb{O}$ represents a set of RGB pixel-valued image observations. There are K transition functions, $T_k : \mathbb{S} \times \mathbb{A} \times \mathbb{S} \to [0, 1]$, each of which describing the environment dynamics $p_k(s_{t+1}|s_t, a_t)$, as well as the reward function $R : \mathbb{S} \times \mathbb{A} \to \mathbb{R}$. Finally, Z creates links from the states to the observations, i.e., $Z : \mathbb{S} \times \mathbb{O} \to [0, 1]$. We aim to optimize a policy π, taking states as inputs and outputs actions, to maximize the expected return $\mathbb{E}[\Sigma_{t \geq 0} \gamma^t r_t]$, with r_t being the reward at time t and $\gamma \in [0, 1]$ being the discount factor.

3.1 Background

World models (Ha & Schmidhuber, 2018a;b) are "generative models of environments" (Alonso et al., 2024). The world model's objective is to learn a probabilistic mapping of the environmental dynamics, $p(s_{t+1}, r_t|s_t, a_t)$, using the past traces of an agent's interactions with the environment. As the world model closely approximates the real environment, it can accurately infer both future observations and reward signals that the environment is likely to generate from a specific sequence of actions. By repeating this inference procedure over multiple time steps in an autoregressive manner, one can derive virtual rollouts of the future, commonly and conveniently referred to as imagination (Hamrick, 2019).

From the perspective of policy learning, the practical merit of using well-trained world models is sample efficiency. As long as the world model closely reproduces the environment, an agent becomes capable of optimizing a policy solely within the imagination unrolled by the world model without needing to adjust its policy directly through repetitively making trials and errors in the real environment. Interacting with the environment is necessary only to formulate and solidify the world model.

The standard formulation (Ha & Schmidhuber, 2018a) of the world model comprises three distinctive modules: 1) a visual sensory component V that encodes high-dimensional observations into stochastic latent embeddings, 2) a memory component M that predicts the future given the past traces of observation-action-reward triplets, and 3) a decision-making component C that optimizes the policy inside the imagination MDP, i.e., the virtual rollouts generated by M and V up to a finite imagination horizon.

3.2 World model formulation

We present a world model formulation designed to capture the diverse dynamics of Atari environments with sufficient fidelity to enable seamless zero-shot policy transfer from the world model to the real environments. Adhering to the standard paradigm (Ha & Schmidhuber, 2018b), our framework decomposes the agent into the three aforementioned distinct components. To this end, we follow the standard world-modeling scheme.

Visual sensory component (V). Following the formulation in Ha & Schmidhuber (2018a), we employ a vanilla variational autoencoder (VAE) (Kingma & Welling, 2014; Rezende et al., 2014) that compresses high-dimensional observations into a compact, continuous latent space modeled by multivariate Gaussian distributions. VAE encodes observations into the latent embeddings, i.e., $z_t \sim q_\phi(z_t|o_t)$, with $q_\phi(z_t|o_t)$ being the recognition model, i.e., the variational distribution that approximates the underlying posterior and ϕ being the neural network parameterization. To permit gradient-based optimization through this stochastic node, VAE adopts the reparameterization trick, expressing z_t as a deterministic transformation of the encoder outputs and independent noise. Subsequently, the probabilistic decoder corresponds to $o_t \sim p_\theta(o_t|z_t)$, with θ being the respective set of neural network parameters of the decoder. Here, a single VAE encoder encodes the observations generated by multiple environments. Refer to Appendix B for comprehensive details on model architecture, training configurations. We provide comparisons with alternative visual backbones used in comparable world model approaches that are operationalized on the Atari 100k benchmark in Appendix B.1.

Memory component (M). We adopt a GPT-style (Radford et al., 2019) decoder-only transformer (Vaswani et al., 2017) as the architectural backbone of the memory component, with the latent embedding dimensionality of d and L layers. The model processes a sequential trajectory of triplets (z_t, a_t, r_t), where z_t is the continuous latent embedding sampled from the VAE, a_t is the discrete action token, and r_t is the reward. Following prior approaches (Micheli et al., 2023; Alonso et al., 2024), we discretize the reward signal by applying the sign function to $\{-1, 0, 1\}$ and combining it with the termination signal, resulting in a vocabulary of six distinct categories. This formulation necessitates a hybrid modeling approach, handling continuous latent embeddings z_t alongside discrete tokens representing both actions and rewards.

To predict the next latent state z_t, we first compute the contextualized transformer representation at the reward token of the previous time step r_{t-1}:

$$h(r_{t-1}) = \textsc{Transformer}(z_{<t}, a_{<t}, r_{<t}).$$

We then pass this context vector through a multi-layer perceptron (MLP) projection head to compute the estimate $\hat{z}_t = \mathrm{MLP}(h(r_{t-1}))$, minimizing the Mean Squared Error (MSE) between z_t and $\hat{z}_t$. Subsequently, to predict the current reward r_t, we compute the context vector at the current action a_t, which incorporates the information from the current latent state:

$$h(a_t) = \textsc{Transformer}(z_{\leq t}, a_{\leq t}, r_{<t}).$$

This is passed to an MLP to compute the estimate $\hat{r}_t = \mathrm{MLP}(h(a_t))$, which is optimized using cross-entropy (CE) loss. The final training objective is a weighted sum of these components, computed as $\mathcal{L} = \mathcal{L}_{\mathrm{MSE}} + \alpha \cdot \mathcal{L}_{\mathrm{CE}}$, where α is a configurable scalar hyperparameter regulating the trade-off. Refer to Appendix C for additional details on the transformer world model backbone.

Decision-making component (C). Policy optimization occurs entirely within the imagined MDPs. While the memory component predicts the environmental dynamics $(\hat{z}_t, \hat{r}_t)$, the policy π determines the action a_t. We project the predicted latent state $\hat{z}_t$ to an observation embedding $\hat{o}_t$ via an MLP from the transformer and apply frame stacking to capture temporal context:

$$\hat{o}_t = \mathrm{MLP}(\hat{z}_t), \quad a_t \sim \pi(a_t \mid \hat{o}_{\leq t}).$$

Distinct from prior works utilizing Soft Actor-Critic or Dreamer-style objectives, we employ Proximal Policy Optimization (PPO) (Schulman et al., 2017). This choice is strategic: since the expert data was generated via PPO, retaining the identical algorithmic structure isolates world model fidelity as the sole variable of interest. This allows us to rigorously assess whether the learned dynamics are accurate enough to recover the expert's performance upper bound without algorithmic and structural confounds. Refer to Appendix A for implementation details on the presupposed, expert PPO policy.

Remark. We emphasize that the adoption of this *minimalist design philosophy*—eschewing complex auxiliary objectives or domain-specific inductive biases—is a deliberate design choice. Our primary objective is to investigate the feasibility of a *unified* world model capable of generating imaginary MDPs with sufficient fidelity across multiple Atari environments, constrained by a limited data budget of 100k samples per task. By stripping the architecture down to its essentials and employing standard off-the-shelf components, we establish a clean, controlled setting to isolate the fundamental effects of model scale and task complexity on capturing both environment-specific dynamics and general intricacies that permeate all games. This ensures that the observed capabilities of the unified agent are attributable to the underlying capacity of the model rather than architectural idiosyncrasies. Throughout our experiments and in Appendix B, we empirically validate that this minimalist setup suffices to resolve essential visual details and dynamics, enabling the policy learned solely within the world model to asymptotically recover the performance upper bound of the offline dataset, on which the world model itself was formulated, when deployed in the real environment.

4 Experiments

4.1 Experimental setup

Construction of the offline data testbed. We construct a fixed offline dataset to formulate and evaluate both environment-wise individual and unified world models. Adhering to the data budget constraints of the Atari 100k benchmark (Łukasz Kaiser et al., 2020), we limit the interaction history for each of the 26 environments to 400k environmental steps. With a standard frame-skip parameter of 4, this amounts to 100k transitions, stored as quadruplets of observation, action, reward, and termination signals. Unlike the standard online setting, where agents continuously update their policies against the real environment, our protocol restricts the world model to this static dataset. This design creates a controlled testbed to rigorously assess whether model scaling alone can capture the diverse dynamics required for generalist performance.

Dataset composition and the presupposed policy. The composition of this offline dataset is critical. A dataset collected via purely random policies fails to traverse the later stages of complex, multi-stage games such as Hero, Frostbite, or Qbert, effectively depriving the world model of the experience required to model downstream environmental progression. Conversely, a dataset collected exclusively by a deterministic expert policy lacks the necessary stochasticity; a world model trained on such narrow trajectories typically collapses when the imaginary agent deviates even slightly from the expert's path. To balance the need for deep state-space coverage with robust error recovery, we employ a policy-based data collection strategy using the Proximal Policy Optimization (PPO) algorithm (Schulman et al., 2017). We train these PPO agents from scratch for all 26 environments rather than using publicly available checkpoints. This decision is twofold: first, it ensures complete coverage of all 26 games; second, and more importantly, it allows us to enforce an identical architectural configuration for both the data-collecting PPO and the policy optimization algorithm used later inside the world model. By aligning the model structures, we eliminate potential confounding variables arising from algorithmic discrepancies, allowing us to verify the degree to which the world model can recover the asymptotic performance upper bound of the original data collection policy.

Collection schedule and stochasticity injection. To capture a comprehensive range of environmental dynamics, we implement a collection schedule with gradually decreasing stochasticity. Using the pre-trained PPO checkpoints, we collect trajectories where the agent selects a random action with probability p_{rand} and follows the expert policy otherwise. The noise parameter decays according to the schedule $p_{\text{rand}} = 1 - \frac{\log_{10}(1+i)}{5}$ at collection step i, transitioning from high-entropy exploration in the early phase to near-deterministic expert behavior as i approaches 100k. Configuration details on the PPO training hyper-parameters, specific operation conditions, and environmental preprocessing are provided in Appendix A.

Configurations. Detailed model and training configurations, learning curves, and the encode-decode results on the 26 Atari gaming environments are covered in Appendix B. The model and training configurations, as well as the environment-wise learning curves, are disclosed in Appendix C.

4.2 Results on individual world models

We analyze the performance of individually trained world models, denoted as $\mathcal{W}_{\text{ind}}^{(\text{Env})}$, where the superscript specifies the target environment (e.g., $\mathcal{W}_{\text{ind}}^{(\text{Alien})}$). Our objective is to characterize how diverse environmental dynamics interact with fixed model capacities. Specifically, we investigate whether different gaming environments exhibit distinct scaling behaviors—effectively occupying different parameterization regimes—despite sharing identical data budgets and architectural configurations. We hypothesize that these variations are attributable to the differing *intrinsic dimensionalities* inherent to the visual and dynamical complexity of each game. To empirically verify this, we train transformer world models for each environment with a fixed embedding dimension of 512 while varying the network depth $L \in \{2, 4, 8, 12, 24, 48, 96\}$. This sweep results in a linear progression of model capacity, ranging from approximately 6 million to 300 million parameters.

Figure 2 visualizes this landscape. The top panels illustrate the schematic of the deep double Descent phenomenon (Nakkiran et al., 2021), mapping generalization risk against relative model complexity. In the

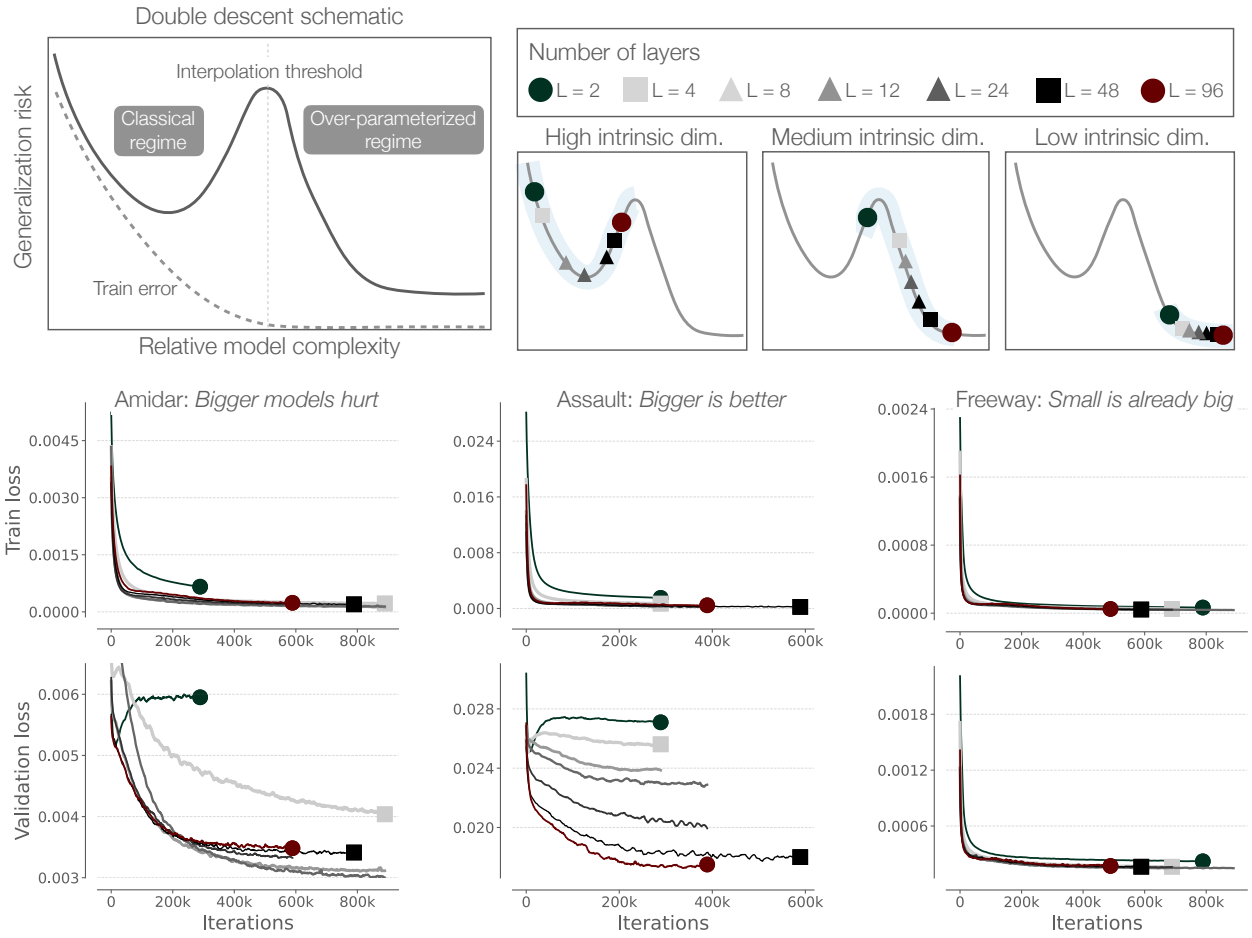

Figure 2: **(Top left)** Schematic of the deep double descent phenomenon with the generalization risk peaking at the interpolation threshold, which dichotomizes the classical and modern overparameterized regimes. **(Top right)** Divergent generalization regimes. Even with the identical sample budget ($N = 10^5$) and model configurations ($L = 2 \ldots 96$), increasing model size yields different trends depending on task complexity. High-complexity tasks remain in the classical regime (*Bigger models hurt*), medium-complexity tasks benefit from over-parameterization (*Bigger is better*), and low-complexity tasks saturate immediately (*Small is already big*). **(Bottom)**: Empirical loss curves. Model depths are distinguished by colors and markers, from $L = 2$ (green circle), $L = 4$ (light gray square), up to $L = 48$ (black square), $L = 96$ (red circle). Validation trends of three different Atari environments confirm the three aforementioned regimes: for high-complexity tasks (Amidar), larger models generalize worse, with $L = 8$ outperforming $L = 96$; for medium-complexity tasks (Assault), performance improves monotonically with model size; and for low-complexity tasks (Freeway), curves overlap, indicating saturation at $L = 4$. We present results averaged across three independent runs and use a α-trimmed mean filter with $\alpha = 0.2$ and a window size of 10.

classical regime, increasing model capacity initially reduces bias but eventually leads to variance-dominated overfitting, characterized by a peak in the generalization risk at the interpolation threshold. Beyond this lies the over-parameterized regime where increasing model size further acts as a robust regularizer, driving generalization risk down once again. Crucially, for a fixed-size offline dataset, the position of this interpolation threshold is dictated by the intrinsic dimensionality of the underlying task. Consequently, identical model architectures applied to different environments may occupy entirely different parameterization regimes.

The bottom panels of Figure 2 confirm this hypothesis by analyzing representative environments for high, medium, and low intrinsic dimensionalities. We observe distinct scaling behaviors for each category:

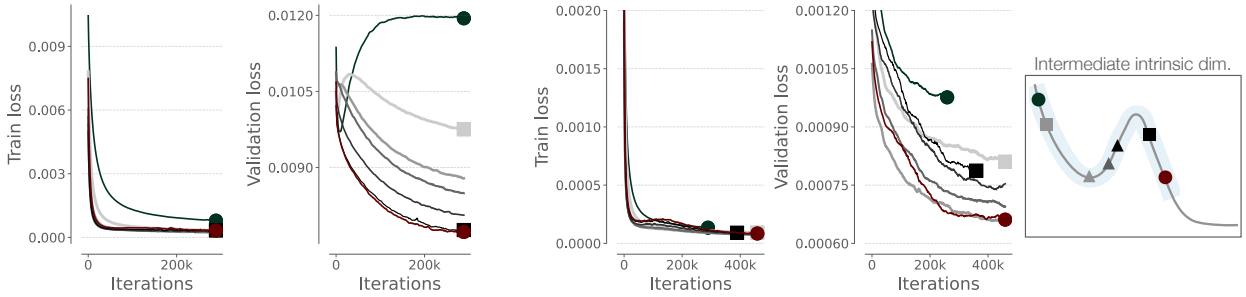

Figure 3: **(Left)** Average loss curves across 26 separately-trained transformer world models, each with its corresponding Atari environment. The global trend shows monotonic improvement with model depth, driven by the prevalence of medium-complexity tasks (12/26) (see Table 1) where over-parameterization is strictly beneficial. **(Right)** Training dynamics for Pong (intermediate intrinsic dimension). It reveals the canonical double descent trajectory: validation loss initially improves ($L = 2 \to 8$), deteriorates as it reaches the interpolation threshold ($L = 12 \to 48$), and recovers to achieve the lowest validation loss in the highly over-parameterized regime ($L = 96$). We present results averaged across three independent runs and use a α-trimmed mean filter with $\alpha = 0.2$ and a window size of 10.

High intrinsic dimensionality: *Bigger models hurt.* In high-complexity environments such as Amidar, the task complexity exceeds the effective capacity of even the largest model of $L = 96$ relative to the limited data to reach the interpolation threshold. While the training loss effectively reaches zero for models with $L \geq 4$, the validation loss exhibits a classical U-shaped curve. The intermediate models ($L = 8$ to $L = 12$) achieve the lowest validation loss, whereas further increasing depth to $L = 24, 48$, and 96 leads to degradation in fidelity. The models remain in the classical overfitting regime; the interpolation threshold has not yet been surpassed, and thus, adding parameters is detrimental to generalization.

Medium Intrinsic Dimensionality: *Bigger is better.* Environments with moderate complexity, such as Assault, reside squarely in the modern over-parameterized regime. Here, we observe a monotonic improvement in validation performance as model depth increases. Unlike the high-complexity cases, even the smallest models in our sweep possess sufficient capacity to surpass the interpolation threshold. Consequently, further increasing the model size does not lead to overfitting; instead, the additional capacity serves to reduce variance and smooth the decision boundary, leading to strictly beneficial scaling behavior.

Low intrinsic dimensionality: *Small is already big.* Finally, low-complexity environments such as Freeway exhibit rapid saturation. Because the underlying dynamics are simplistic, even the shallower models (e.g., $L = 4$) effectively capture the data manifold. Consequently, the validation loss curves for larger models ($L = 8$ through $L = 96$) essentially overlap with no significant gain. In this regime, the task is solved by minimal capacity, rendering further scaling redundant though not harmful.
The right panels of Figure 3 depict the average loss curves aggregated across all 26 individually trained world models. For the complete set of empirical loss curves for every specific environment, refer to Figure 12 in the Appendix. The global average follows the trend of the medium intrinsic dimensionality regime, indicating that, in aggregate, the benefits of scaling outweigh the costs within our parameter sweep up to $L = 48$.

Notably, the left panels of Figure 3 reveal a distinct trend falling outside the previously defined categories:

Intermediate Intrinsic Dimensionality: *Bigger hurts, then helps.* In environments exemplified by Pong, the task complexity is adequately positioned relative to our model sweep to manifest the full double descent phenomenon, spanning both classical and over-parameterized regimes. Initially, we observe standard classical behavior: increasing model depth from $L = 2$ to $L = 8$ reduces bias, leading to an improvement in validation loss. However, as we push beyond this local optimum into the critical regime ($L = 12$ to $L = 48$), the trend reverses. Here, the model capacity becomes just large enough to interpolate the training noise but is insufficient to smooth the decision boundary, causing variance to dominate and performance to deteriorate. Crucially, as we further scale into the highly over-parameterized regime ($L = 96$), the validation risk declines

Table 1: Categorization of Atari environments by the generalization regime. We categorize 26 games into four regimes based on the alignment of the interpolation threshold relative to our model sweep ($L = 2 \ldots 96$) (see Figure 2). This reveals a spectrum of effective task complexity, ranging from HIGH (classical overfitting) to LOW (immediate saturation).

Intrinsic Dim.	Count	Generalization Trend	Environments
HIGH	6	*Bigger models hurt*	Alien, Amidar, Breakout, Gopher, Kangaroo, MsPacman
INTERMEDIATE	2	*Bigger hurts, then helps*	Pong, Qbert
MEDIUM	12	*Bigger is better*	Assault, Asterix, Boxing, ChopperCommand, CrazyClimber, DemonAttack, Hero, Jamesbond, Krull, PrivateEye, RoadRunner, UpNDown
LOW	6	*Small is already big*	BankHeist, Battlezone, Freeway, Frostbite, KungFuMaster, Seaquest

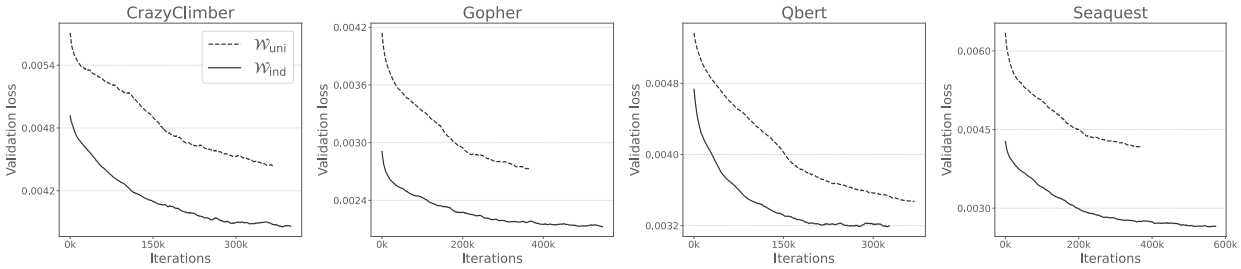

Figure 4: Validation loss comparison between the unified model $\mathcal{W}_{\text{uni}}$ (dashed) and individual models $\mathcal{W}_{\text{ind}}$ (solid) with fixed capacity ($L = 24$) across four representative environments. The specialist $\mathcal{W}_{\text{ind}}$ consistently outperforms the generalist $\mathcal{W}_{\text{uni}}$. This gap illustrates capacity dilution: whereas $\mathcal{W}_{\text{ind}}$ optimizes for a single manifold, $\mathcal{W}_{\text{uni}}$ must amortize its resources across 26 distinct distributions, thereby increasing error.

once again, eventually surpassing the performance of the classical best ($L = 8$). This complete trajectory—where scaling is first beneficial, then detrimental, and finally restorative—justifies the designation of the *canonical double descent*, confirming that while intermediate scaling hurts, extreme scaling helps.

Table 1 provides a systematic categorization of all 26 Atari environments. We classify each game into one of the four generalization regimes based on the specific alignment of its interpolation threshold relative to our fixed model capacity sweep. Refer to Appendix D for our qualitative interpretation regarding the categorization of each gaming environment into distinct intrinsic dimensionality regimes. Finally, we verify that the performance degradation observed in the high intrinsic dimensionality regime is strictly attributable to classical overfitting rather than training instability. While prior literature reports that scaling transformer depth can frequently lead to gradient divergence or attention entropy collapse (Li et al., 2020; Zhai et al., 2023), our deepest models ($L = 96$) consistently achieve near-zero training error across all environments (see Figure 2, bottom panels). This decoupling of training and validation trends confirms that the degradation is a result of high variance (generalization gap) rather than optimization failure. Furthermore, to rule out the influence of stochastic noise, all reported curves in the main body represent the mean performance averaged over three independent random seeds.

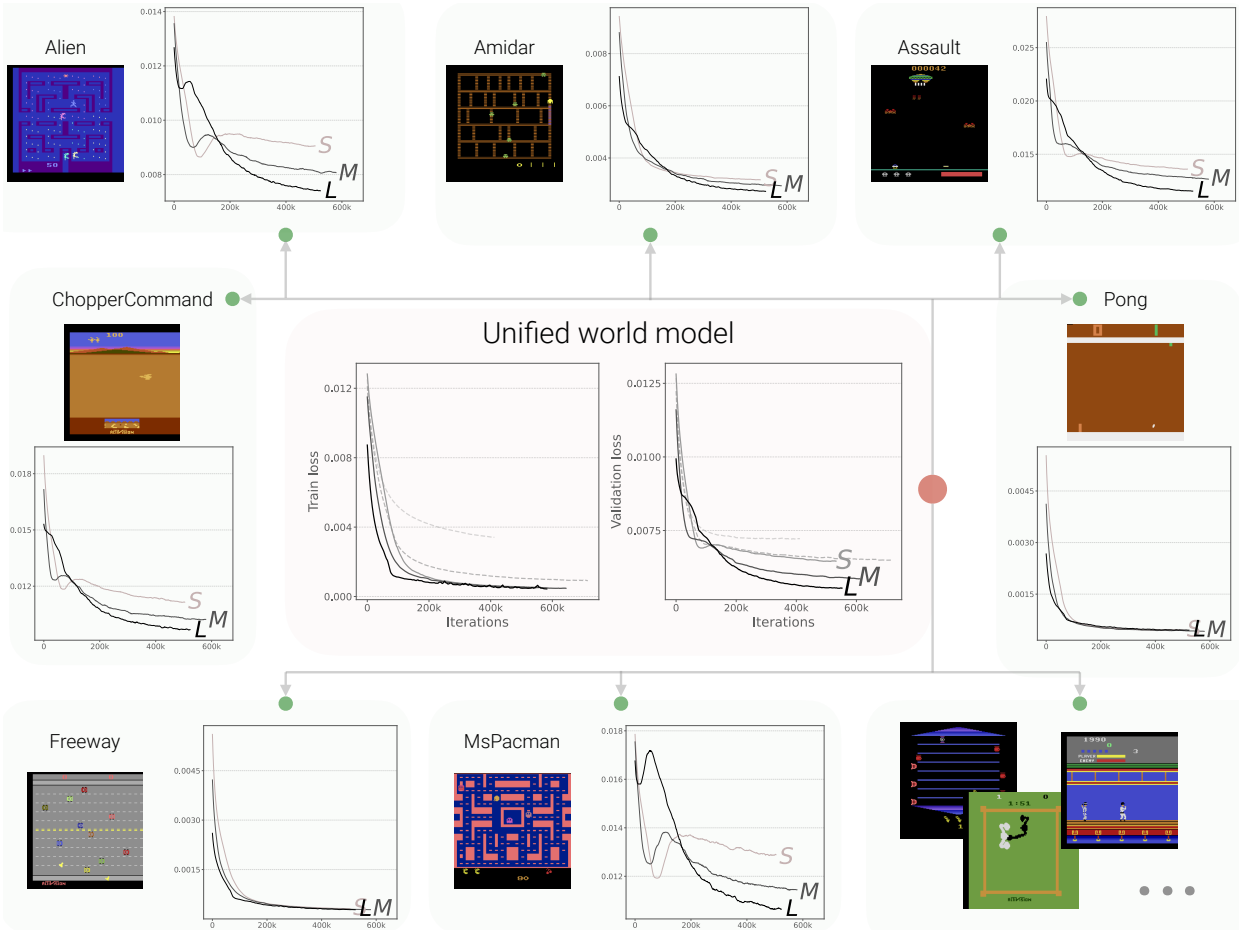

Figure 5: Learning dynamics of the unified world model $\mathcal{W}_{\text{uni}}$. We display aggregated and environment-wise learning curves for a single model instance trained simultaneously on all 26 Atari environments. **(Center)** Solid lines correspond to Small (S), Medium (M), and Large (L) configurations that possess sufficient capacity to reach the interpolation threshold, i.e., achieving near-zero training loss. Dashed lines represent underparameterized models, which converge to significantly higher loss values. **(Surrounding Panels)** Validation loss curves for 7 representative environments (selected from the full set of 26 due to space limits). We observe that within this unified training setup, performance monotonically improves or stabilizes with scale, confirming that *bigger models never hurt*. This stands in contrast to individual-environment training results, where increasing model capacity often leads to performance deterioration in environments with high or intermediate intrinsic dimensionality regimes, e.g., Alien, Amidar (Figure 2) or Pong (Figure 3).

4.3 Results on unified world models

We now evaluate the unified world model, $\mathcal{W}_{\text{uni}}$, a single transformer trained simultaneously on the aggregated dataset of all 26 Atari environments. Our objective is to determine how scaling laws evolve when transitioning from modeling isolated environments to a vast, heterogeneous joint distribution.

First, we quantify the performance trade-off between specialist and generalist models. Figure 4 contrasts the validation loss of the unified model against individual baselines across four representative environments with fixed capacity (latent dimensionality 512, 24 layers). We observe that $\mathcal{W}_{\text{ind}}$ consistently achieves lower validation loss than $\mathcal{W}_{\text{uni}}$. This phenomenon, known as *negative transfer* (Standley et al., 2020), is structurally expected: whereas the individual model dedicates its entire parameter budget to the idiosyncrasies of a single game, the unified model must amortize its capacity across 26 disjoint dynamical systems. Consequently, for a fixed parameter count, the generalist inevitably incurs a higher reconstruction error than the specialist.

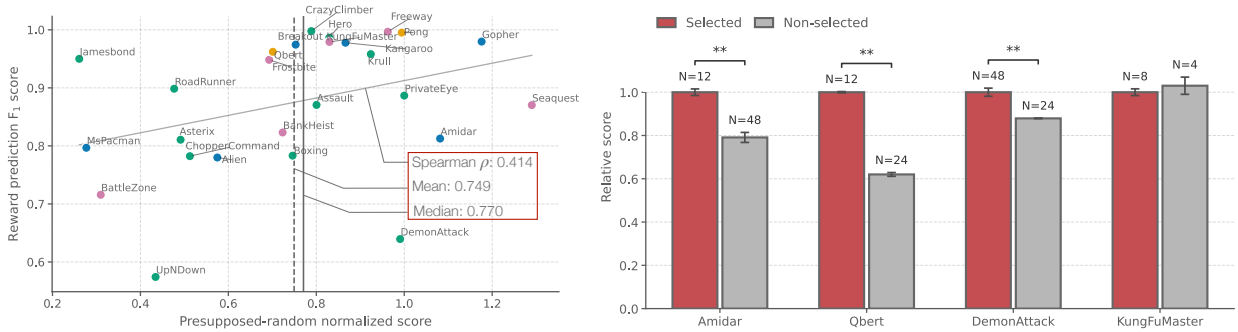

Figure 6: Downstream policy performance in learned environments. **(Left)** Normalized scores for 26 environments vs. reward predictor F_1 score. The mean (0.749) and median (0.770) scores confirm sufficient fidelity for agent training, while the correlation ($\rho = 0.414$) indicates performance is partly bounded by reward accuracy. **(Right)** Policy performance of optimally scaled (Selected) vs. baseline (Non-selected) models (mean $\pm$ SE over 16 independent trials). Other than for the saturated low-complexity case (KungFuMaster), matching model capacity to intrinsic dimensionality yields significant gains ($p < 0.01$), confirming validation world model loss as a robust proxy for downstream policy-learning.

Positive regularization: *Bigger models never hurt* While the unified model incurs a performance penalty due to negative transfer, it offers a critical countervailing advantage through what we term *positive regularization*, which ensures scaling stability. Figure 5 presents the learning dynamics of $\mathcal{W}_{\text{uni}}$ across five model configurations, ranging from under-parameterized baselines ($L = 8$, $d \in \{512, 1024\}$; dashed lines) to over-parameterized networks ($L \in \{4, 8, 24\}$, $d = 2048$; solid lines, denoted as S, M, L, respectively), with the largest configuration reaching approximately 1.2 billion parameters. Refer to Appendix G for the full results.

Remarkably, once $\mathcal{W}_{\text{uni}}$ enters the over-parameterized regime, we observe that *bigger models consistently improve or sustain performance*, evaluated on all environments. This stands in distinct contrast to the individual experiments ($\mathcal{W}_{\text{ind}}$, subsection 4.2), where high- or intermediate-complexity environments (e.g., Alien, Pong) required precise architectural tuning to avoid entering the critical regime of degradation. In the unified setting, we observe that the joint distribution acts as a robust regularizer, effectively mitigating the inverted-U overfitting curve observed in isolated training. We posit that this reframes the standard multi-task learning narrative. While the literature often focuses on the detriment of *negative transfer*, our results highlight the distinct mechanism of *positive regularization*: the task diversity protects individual environments from overfitting, supporting a "scale-first" strategy where model capacity can be increased with significantly reduced risk of degradation.

4.4 Results on policy learning in world models

Having established that appropriate scaling is crucial for enabling world models to faithfully mirror the real environment—either by tuning individual capacities to their intrinsic dimensionalities or by leveraging positive regularization through training a unified model—we now address the logical subsequent question: does this improved fidelity translate to effective downstream policy learning? The central premise of our minimalist design is to emphasize the primacy of scale over structural sophistication. However, this hypothesis holds only if the resulting world models possess sufficient fidelity to support the training of competent agents. To rigorously test this, we evaluate PPO agents trained entirely within the *learned* dynamics of our best-performing individual world models. Crucially, the performance of these agents is bounded by that of the *presupposed* expert PPO policy used to collect the offline dataset. To ensure a strictly controlled comparison, we maintain the training configuration of the in-model agents—including network architecture, learning rate, and total optimization steps—identical to that of the expert presupposed agent, varying only the rollout horizon (32 vs. 128) while compensating with a quadrupled batch size to maintain parity in total environmental steps. To isolate the impact of transition dynamics from reward modeling, we deploy an

external, independent reward predictor, also trained from the limited offline dataset, for each environment, held constant across all world model configurations (see Appendix E). This setup isolates the fidelity of the world model as the sole variable, allowing us to determine if properly scaled minimalist models can serve as effective surrogates for the real environment.

Figure 6 (left) summarizes the performance of policies trained within our best-performing individual world model configurations across all 26 environments. Refer to Appendix H for the learning curves inside the world models. We plot the normalized policy score (x-axis)—scaled such that 0 corresponds to a random agent and 1 to the presupposed expert—against the F_1 score of the external reward predictor (y-axis). The results demonstrate strong transfer fidelity: we achieve a median normalized score of 0.770 and a mean of 0.749, indicating that the minimalist world models successfully capture the critical dynamics required to recover approximately 75% of the expert's performance. Notably, in environments such as Amidar, Gopher, and Seaquest, the agents trained inside the world model exceed the performance of the presupposed policy used to generate the data. Furthermore, the scatterplot reveals a positive correlation (Spearman's $\rho = 0.414$) between reward prediction accuracy and policy performance. This suggests that in cases where performance lags, the limitation often stems from the external reward signal rather than the fidelity of the transition dynamics. Overall, these findings confirm that when scaled correctly to match the intrinsic dimensionality of the environment, minimalist world models serve as effective surrogates for the real environment.

Finally, we examine whether the validation loss improvements achieved through specific scaling strategies translate into statistically significant differences in policy performance. Figure 6 (right) compares the normalized scores of policies trained in the optimally scaled world models (Selected) against those trained in standard baseline configurations (Non-selected) across four representative environments. For high-complexity environments like Amidar and intermediate cases like Qbert, where smaller models ($L = 12$) outperformed larger baselines ($L = 48, 24$) in validation loss, we observe a corresponding significant advantage in downstream policy performance ($p < 0.001$). Conversely, for DemonAttack, where the intrinsic dimensionality supports the *Bigger is Better* trend, the larger model ($L = 48$) significantly outperforms the medium baseline ($L = 24$). The only exception is the low-complexity environment KungFuMaster, where performance saturates early; here, both the small ($L = 8$) and very small ($L = 4$) models achieve similar degree of expert recovery with no significant difference. These results, averaged over 16 independent trials with error bars representing the standard error, confirm that the intrinsic dimensionality regimes identified via validation loss are predictive of downstream task success. This underscores that correct model scaling is not merely a metric-optimization exercise but a prerequisite for learning functional policies.

5 Discussion and Conclusion

In this work, we isolated the impact of scale in transformer world models, demonstrating that performance is not merely a function of architectural priors but is strictly governed by the interplay between model capacity and environmental intrinsic dimensionality. Our analyses identified distinct scaling regimes: individual models frequently encounter performance degradation in complex environments due to capacity saturation, exhibiting an inverted-U curve. In contrast, we found that unified training induces *positive regularization*, effectively stabilizing scaling dynamics and ensuring monotonic improvements across all tasks regardless of their complexity. This suggests that the diversity of a multi-task dataset acts as a regularizer, allowing larger models to generalize better than their specialist counterparts with enough degree of scaling. We further confirmed that this improved fidelity directly enables high-performing policies learned in imagination.

Future research should extend this analysis to environments necessitating long-horizon reasoning. Moreover, while this work focused on offline datasets, a truly generalist agent must operate in a conventional iterative setting: progressing from random actions to world model formulation, policy optimization, and subsequent data collection in a continuous loop. This shift introduces the challenge of non-stationary data distributions, where maintaining the model's ability to adapt becomes paramount; effectively mitigating the loss of plasticity (Dohare et al., 2024) will be essential for sustained learning. Finally, although we employed separate policy heads for evaluation, the ultimate goal is a single, unified controller. Achieving this will likely require scaling the policy networks in tandem with the world model, utilizing the same principles of positive regularization to master diverse dynamics across diverging environments.

References

Pranav Agarwal, Sheldon Andrews, and Samira Ebrahimi Kahou. Learning to play Atari in a world of tokens. In *ICML*, 2024. URL https://proceedings.mlr.press/v235/agarwal24b.html.

Eloi Alonso, Adam Jelley, Vincent Micheli, Anssi Kanervisto, Amos Storkey, Tim Pearce, and François Fleuret. Diffusion for world modeling: Visual details matter in Atari. In *NeurIPS*, 2024. URL https://openreview.net/forum?id=NadTwTODgC.

Yoshua Bengio, Nicholas Léonard, and Aaron Courville. Estimating or propagating gradients through stochastic neurons for conditional computation. *arXiv preprint arXiv:1308.3432*, 2013. URL https://arxiv.org/abs/1308.3432.

Rishi Bommasani, Drew A Hudson, Ehsan Adeli, Russ Altman, Simran Arora, Sydney von Arx, Michael S Bernstein, Jeannette Bohg, Antoine Bosselut, Emma Brunskill, et al. On the opportunities and risks of foundation models. *arXiv preprint arXiv:2108.07258*, 2021. URL https://arxiv.org/abs/2108.07258.

Maxime Burchi and Radu Timofte. Learning transformer-based world models with contrastive predictive coding. In *ICLR*, 2025. URL https://openreview.net/forum?id=YK9G4Htdew.

Boyuan Chen, Diego Marti Monso, Yilun Du, Max Simchowitz, Russ Tedrake, and Vincent Sitzmann. Diffusion forcing: Next-token prediction meets full-sequence diffusion. In *NeurIPS*, 2024. URL DiffusionForcing:Next-TokenPredictionMeetsFull-SequenceDiffusion.

Chang Chen, Yi-Fu Wu, Jaesik Yoon, and Sungjin Ahn. Transdreamer: Reinforcement learning with transformer world models. *arXiv preprint arXiv:2202.09481*, 2022. URL https://arxiv.org/abs/2202.09481.

Jie Cheng, Ruixi Qiao, Yingwei Ma, Binhua Li, Gang Xiong, Qinghai Miao, Yongbin Li, and Yisheng Lv. Scaling offline model-based rl via jointly-optimized world-action model pretraining. In *ICLR*, 2025. URL https://openreview.net/forum?id=T1OvCSFaum.

Fei Deng, Junyeong Park, and Sungjin Ahn. Facing off world model backbones: RNNs, transformers, and S4. *arXiv preprint arXiv:2307.02064*, 2023. URL https://arxiv.org/abs/2307.02064.

Zihan Ding, Amy Zhang, Yuandong Tian, and Qinqing Zheng. Diffusion world model: Future modeling beyond step-by-step rollout for offline reinforcement learning. *arXiv preprint arXiv:2402.03570*, 2024. URL https://arxiv.org/abs/2402.03570.

Luke Ditria and Tom Drummond. Long-term prediction of natural video sequences with robust video predictors. *arXiv preprint arXiv:2308.11079*, 2023. URL https://github.com/LukeDitria/CNN-VAE.

Shibhansh Dohare, Fernando Hernandez-Garcia, Qingfeng Lan, Parash Rahman, Rupam Mahmood, and Richard Sutton. Loss of plasticity in deep continual learning. *Nature*, 632:768–774, 2024. URL https://www.nature.com/articles/s41586-024-07711-7.

Albert Gu, Karan Goel, and Christopher Re. Efficiently modeling long sequences with structured state spaces. In *ICLR*, 2022. URL https://openreview.net/pdf?id=uYLFoz1vlAC.

David Ha and Jürgen Schmidhuber. Recurrent world models facilitate policy evolution. In *NeurIPS*, 2018a. URL https://proceedings.neurips.cc/paper_files/paper/2018/file/2de5d16682c3c35007e4e92982f1a2ba-Paper.pdf.

David Ha and Jürgen Schmidhuber. World models. *arXiv preprint arXiv:1803.10122*, 2018b. URL https://arxiv.org/abs/1803.10122.

Danijar Hafner, Timothy Lillicrap, Ian Fischer, Ruben Villegas, David Ha, Honglak Lee, and James Davidson. Learning latent dynamics for planning from pixels. In *ICLR*, 2019. URL https://openreview.net/pdf?id=V6BjBgku7Ro.

Danijar Hafner, Timothy Lillicrap, Mohammad Norouzi, and Jimmy Ba. Mastering Atari with discrete world models. In *ICLR*, 2021. URL https://openreview.net/forum?id=0oabwyZbOu.

Danijar Hafner, Jurgis Pasukonis, Jimmy Ba, and Timothy Lillicrap. Mastering diverse control tasks through world models. *Nature*, pp. 1–7, 2025a. URL https://www.nature.com/articles/s41586-025-08744-2.

Danijar Hafner, Wilson Yan, and Timothy Lillicrap. Training agents inside of scalable world models. *arXiv preprint arXiv:2509.24527*, 2025b. URL https://arxiv.org/abs/2509.24527.

Jessica Hamrick. Analogues of mental simulation and imagination in deep learning. *Current Opinion in Behavioral Sciences*, 29(1):8–16, 2019. URL https://openreview.net/pdf?id=rygPeuADPr.

Jonathan Ho, Ajay Jain, and Pieter Abbeel. Denoising diffusion probabilistic models. In *NeurIPS*, 2020. URL https://dl.acm.org/doi/abs/10.5555/3495724.3496298.

Sepp Hochreiter and Jürgen Schmidhuber. Long short-term memory. *Neural Computation*, 9(8):1735–1780, 1997. URL https://doi.org/10.1162/neco.1997.9.8.1735.

Edward Hu, Qiankun Yang, Alex Lee, Sachin Gurjar, Artur Davari, Philip Garner, Rowan Kwiatkowski, Robert McCutcheon, Fabrizio Bottarel, Simon Peyton-Jones, Bartek Klein, Alex Kendall, and Niels Shahidi. GAIA-1: A generative world model for autonomous driving. *Wayve Research*, 2023. URL https://wayve.ai/thinking/gaia-1-generative-driving-world-model/. Technical Report.

Edward Hu, Qiankun Yang, Alex Lee, Artur Davari, Sachin Gurjar, Philip Garner, Rowan Kwiatkowski, Robert McCutcheon, Fabrizio Bottarel, Simon Peyton-Jones, Bartek Klein, Alex Kendall, and Niels Shahidi. GAIA-2: A controllable, multi-view generative world model for autonomous driving. *Wayve Research*, 2024. URL https://wayve.ai/thinking/gaia-2-multi-view-generative-world-model/. Technical Report.

Eric Jang, Shixiang Gu, and Ben Poole. Categorical reparameterization with Gumbel-softmax. In *ICLR*, 2017. URL https://openreview.net/forum?id=rkE3y85ee.

Leslie Pack Kaelbling, Michael Littman, and Anthony Cassandra. Planning and acting in partially observable stochastic domains. *Artificial Intelligence*, 101(1–2):99–134, 1998. URL https://www.sciencedirect.com/science/article/pii/S000437029800023X.

Diederik Kingma and Max Welling. Auto-encoding variational Bayes. In *ICLR*, 2014. URL https://openreview.net/forum?id=33X9fd2-9FyZd.

Brenden Lake, Ruslan Salakhutdinov, and Joshua Tenenbaum. Human-level concept learning through probabilistic program induction. *Science*, 350(6266):1332–1338, 2015. URL https://www.science.org/doi/10.1126/science.aab3050.

Yann LeCun, Léon Bottou, Yoshua Bengio, and Patrick Haffner. Gradient-based learning applied to document recognition. *Proceedings of the IEEE*, 86(11):2278–2324, 1998. doi: 10.1109/5.726791. URL https://ieeexplore.ieee.org/document/726791.

Kuang-Huei Lee, Ofir Nachum, Mengjiao Sherry Yang, Lisa Lee, Daniel Freeman, Sergio Guadarrama, Ian Fischer, Winnie Xu, Eric Jang, Henryk Michalewski, et al. Multi-game decision transformers. In *NeurIPS*, 2022. URL https://openreview.net/pdf?id=0gouO5saq6K.

Xuezhe Li, Qi Liu, Rod Hauhart, Shinji Matsuzaki, and Noriaki Kawahara. Deep transformers with latent depth. In *NeurIPS*, 2020. URL https://proceedings.neurips.cc/paper/2020/file/1325cdae3b6f0f91a1b629307bf2d498-Paper.pdf.

Haoyu Ma, Jialong Wu, Ningya Feng, Chenjun Xiao, Dong Li, Jianye Hao, Jianmin Wang, and Mingsheng Long. HarmonyDream: Task harmonization inside world models. In *ICML*, 2024. URL https://proceedings.mlr.press/v235/ma24o.html.

Chris Maddison, Andriy Mnih, and Yee Whye Teh. The concrete distribution: A continuous relaxation of discrete random variables. In *ICLR*, 2017. URL https://openreview.net/forum?id=S1jE5L5gl.

Vincent Micheli, Eloi Alonso, and François Fleuret. Transformers are sample-efficient world models. In *ICLR*, 2023. URL https://openreview.net/forum?id=vhFu1Acb0xb.

Vincent Micheli, Eloi Alonso, and François Fleuret. Efficient world models with context-aware tokenization. *arXiv preprint arXiv:2406.19320*, 2024. URL https://arxiv.org/abs/2406.19320.

Preetum Nakkiran, Gal Kaplun, Yamini Bansal, Tristan Yang, Boaz Barak, and Ilya Sutskever. Deep double descent: Where bigger models and more data hurt. *Journal of Statistical Mechanics: Theory and Experiment*, 2021(12):124003, 2021. URL https://doi.org/10.1088/1742-5468/ac3a74.

Ahad Nauman, Marc G. Bellemare, and Marlos C. Machado. Bigger, regularized, categorical: High-capacity value functions are efficient multi-task learners. In *ICLR*, 2024. URL https://openreview.net/forum?id=hXYdI78KqM.

Alec Radford, Jeffrey Wu, Rewon Child, David Luan, Dario Amodei, and Ilya Sutskever. Language models are unsupervised multitask learners. Technical Report 1, OpenAI, 2019. URL https://cdn.openai.com/better-language-models/language_models_are_unsupervised_multitask_learners.pdf.

Jean-François Raskin and Ocan Sankur. Multiple-environment markov decision processes. *arXiv preprint arXiv:1405.4733*, 2014. URL https://arxiv.org/abs/1405.4733.

Scott Reed, Konrad Zolna, Emilio Parisotto, Sergio Gomez Colmenarejo, Alexander Novikov, Gabriel Barth-Maron, Mai Gimeno, et al. A generalist agent. *Transactions on Machine Learning Research*, 2022. URL https://openreview.net/forum?id=135.

Danilo Rezende, Shakir Mohamed, and Daan Wierstra. Stochastic backpropagation and approximate inference in deep generative models. In *ICML*, 2014. URL https://proceedings.mlr.press/v32/rezende14.pdf.

Jan Robine, Marc Höftmann, Tobias Uelwer, and Stefan Harmeling. Transformer-based world models are happy with 100k interactions. In *ICLR*, 2023. URL https://openreview.net/forum?id=TdBaDGCpjly.

John Schulman, Filip Wolski, Prafulla Dhariwal, Alec Radford, and Oleg Klimov. Proximal policy optimization algorithms. *arXiv preprint arXiv:1707.06347*, 2017. URL https://arxiv.org/abs/1707.06347.

Max Schwarzer, Johan Samir Obando Ceron, Aaron Courville, Marc Bellemare, Rishabh Agarwal, and Pablo Samuel Castro. Bigger, better, faster: Human-level Atari with human-level efficiency. In *ICML*, 2023. URL https://openreview.net/pdf?id=2sjm6AH1jB.

Karen Simonyan and Andrew Zisserman. Very deep convolutional networks for large-scale image recognition. *arXiv preprint arXiv:1409.1556*, 2014. URL https://arxiv.org/abs/1409.1556.

Trevor Standley, Amir Zamir, Dawn Chen, Leonidas Guibas, Jitendra Malik, and Silvio Savarese. Which tasks should be learned together in multi-task learning? In *ICML*, 2020. URL https://proceedings.mlr.press/v119/standley20a/standley20a.pdf.

Richard Sutton and Andrew Barto. *Reinforcement Learning: An Introduction*. MIT Press, 1st edition, 1998. ISBN 978-0262193986. URL http://incompleteideas.net/book/the-book.html.

Aaron Van Den Oord, Oriol Vinyals, et al. Neural discrete representation learning. In *NeurIPS*, 2017. URL https://proceedings.neurips.cc/paper_files/paper/2017/file/7a98af17e63a0ac09ce2e96d03992fbc-Paper.pdf.

Ashish Vaswani, Noam Shazeer, Niki Parmar, Jakob Uszkoreit, Llion Jones, Aidan N. Gomez, Lukasz Kaiser, and Illia Polosukhin. Attention is all you need. In *NeurIPS*, 2017. URL https://proceedings.neurips.cc/paper/2017/file/3f5ee243547dee91fbd053c1c4a845aa-Paper.pdf.

Shuangfei Zhai, Tatiana Likhomanenko, Etai Littwin, Dan Busbridge, Jason Ramapuram, Yizhe Zhang, Jiatao Gu, and Joshua M Susskind. Stabilizing transformer training by preventing attention entropy collapse. In *ICML*, 2023. URL https://proceedings.mlr.press/v202/zhai23a/zhai23a.pdf.

Lunjun Zhang, Yuwen Xiong, Ze Yang, Sergio Casas, Rui Hu, and Raquel Urtasun. Copilot4d: Learning unsupervised world models for autonomous driving via discrete diffusion. In *ICLR*, 2024a. URL https://arxiv.org/abs/2311.01017.

Weipu Zhang, Gang Wang, Jian Sun, Yetian Yuan, and Gao Huang. STORM: Efficient stochastic transformer based world models for reinforcement learning. In *NeurIPS*, 2023. URL https://openreview.net/forum?id=WxnrX42rnS.

Weipu Zhang, Gang Wang, Jian Sun, Yetian Yuan, and Gao Huang. STORM: Efficient stochastic transformer based world models for reinforcement learning. In *NeurIPS*, 2024b. URL https://openreview.net/forum?id=WxnrX42rnS.

Łukasz Kaiser, Mohammad Babaeizadeh, Piotr Miłos, Błażej Osiński, Roy Campbell, Konrad Czechowski, Dumitru Erhan, Chelsea Finn, Piotr Kozakowski, Sergey Levine, Afroz Mohiuddin, Ryan Sepassi, George Tucker, and Henryk Michalewski. Model based reinforcement learning for atari. In *ICLR*, 2020. URL https://openreview.net/pdf?id=S1xCPJHtDB.